Electronic Supplementary Material (ESI) for Green Chemistry.

Supporting Information

Enhanced electrocatalytic glucose oxidation assisted hydrogen production via interfacial synergistic effect of $NiO/NiCo_2O_4$ porous nanowire

Zongxi Zhang [a,b], Jiancheng Zhao [a,b], Mei Hong, [a,b] Shuai Chen [* a,b], Yan Qiao [*a,b]

[a] State Key Laboratory of Coal Conversion, Institute of Coal Chemistry, Chinese Academy of Sciences, 27 South Taoyuan Road, Taiyuan 030001, China

[b] Center of Materials Science and Optoelectronics Engineering, University of Chinese Academy of Sciences, Beijing 100049, China

Corresponding Author E-mail: chenshuai@sxicc.ac.cn, qiaoy@sxicc.ac.cn

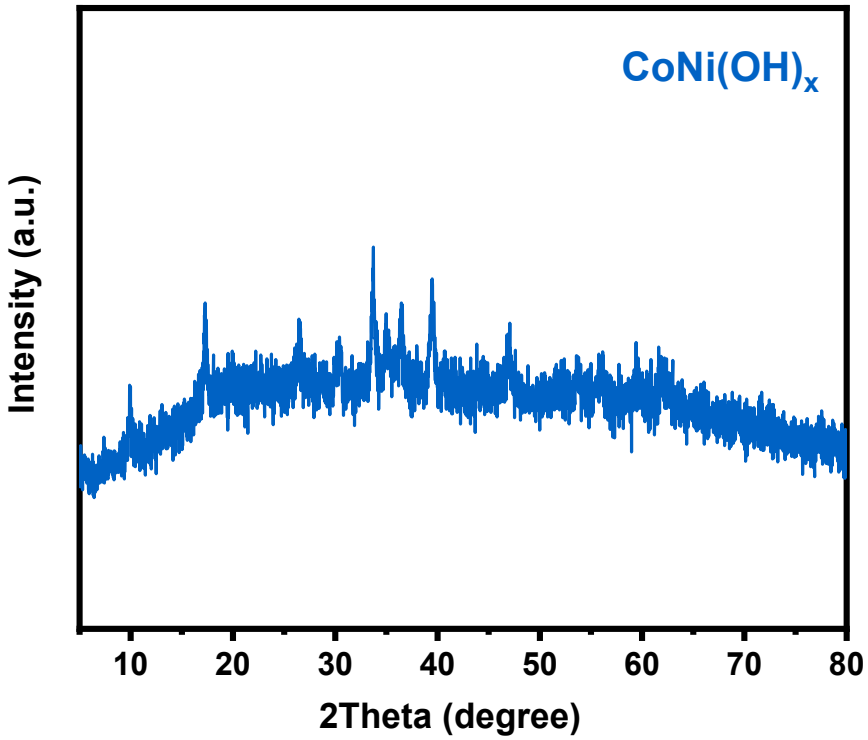

Fig. S1. XRD patterns of $CoNi(OH)_x$.

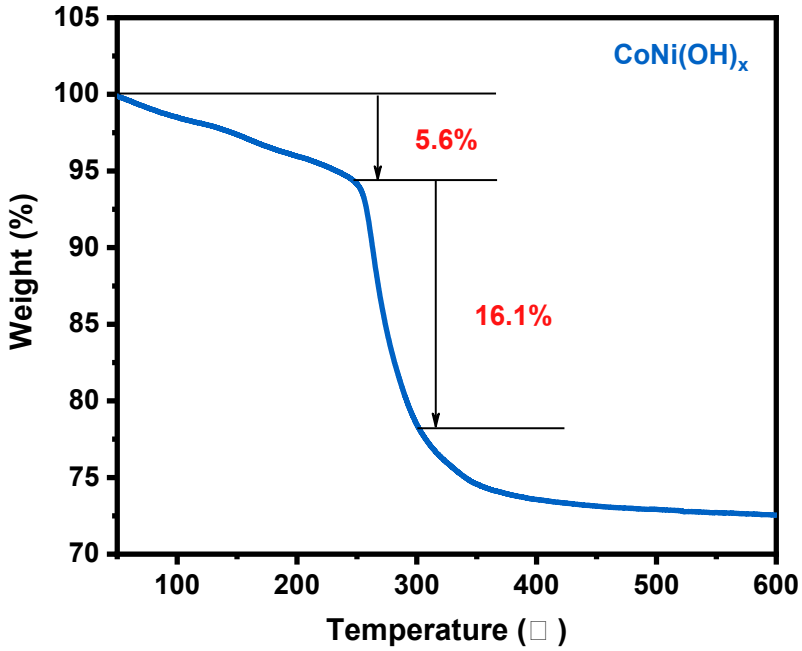

Fig. S2. TG analysis of the $CoNi(OH)_x$.

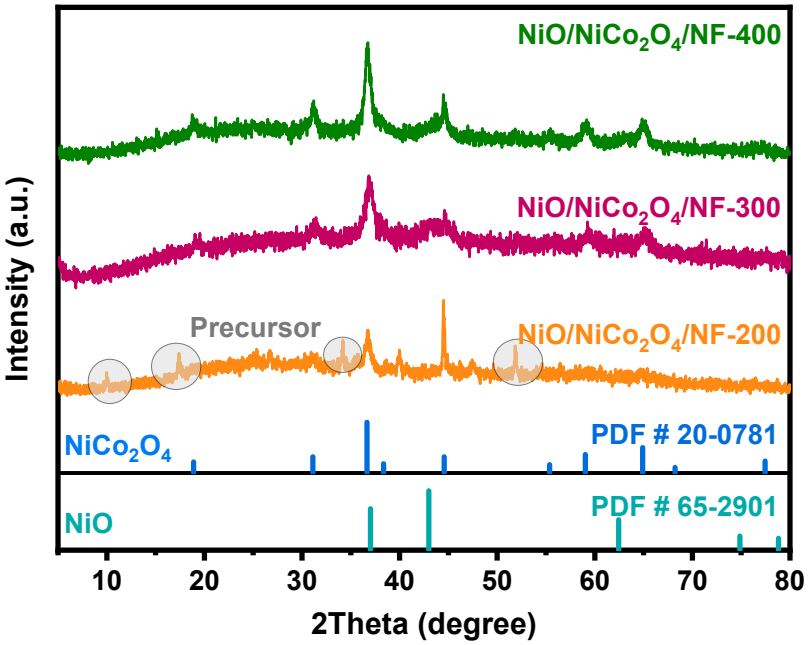

Fig. S3. XRD patterns of $NiO/NiCo_2O_4$/NF-X (X = 200, 300, 400).

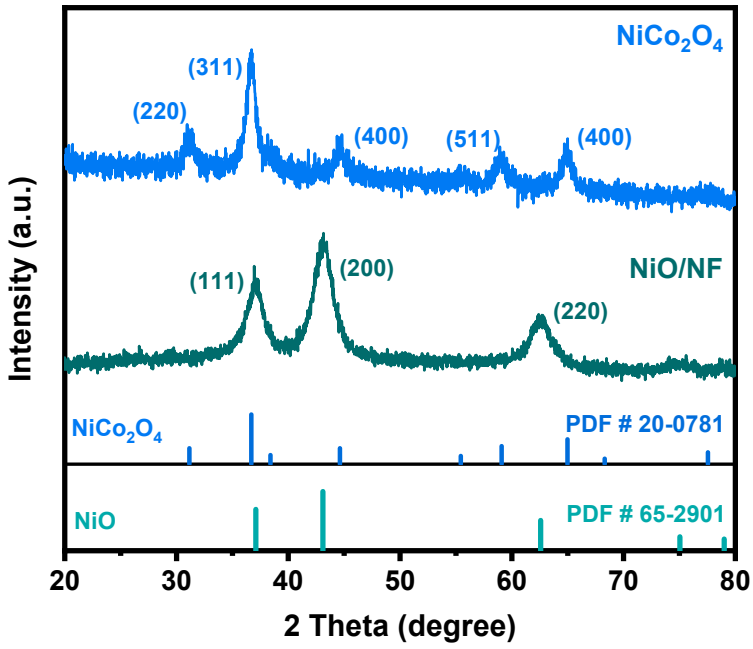

Fig. S4. XRD patterns of NiO/NF and $NiCo_2O_4$.

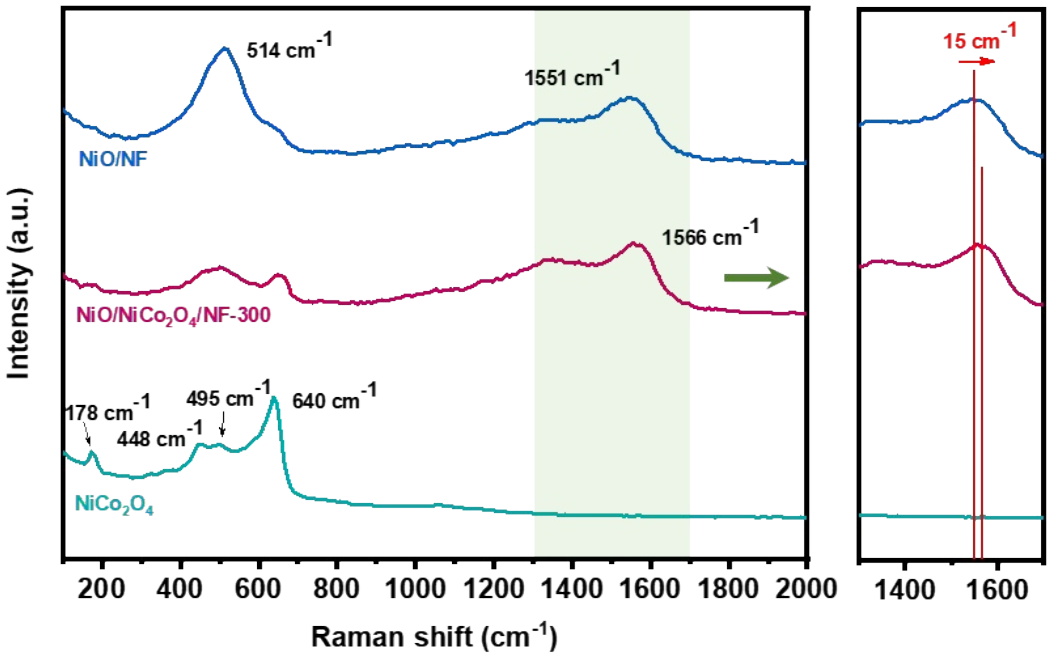

Fig. S5. Raman spectra of $NiCo_2O_4$, $NiO/NiCo_2O_4$/NF-300 and NiO.

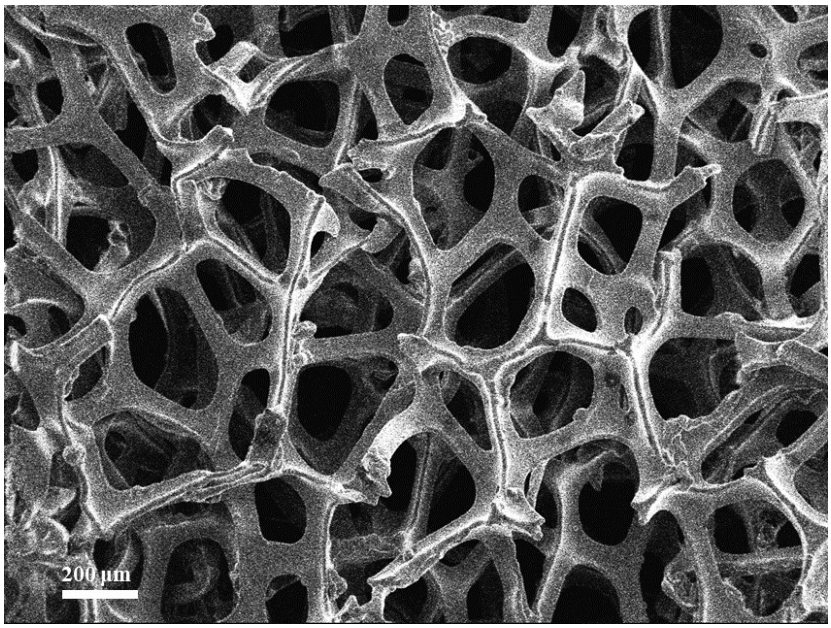

Fig. S6. SEM image of Ni foam.

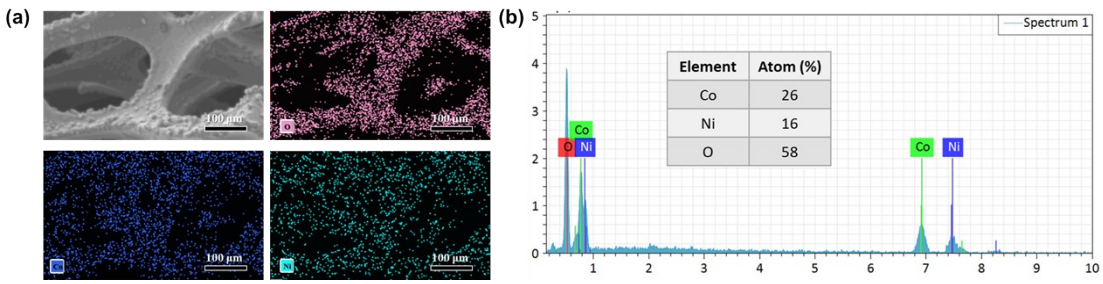

Fig. S7. (a) SEM image, corresponding elements mapping results and (b) the energy dispersive spectroscopy (EDS) of $NiO/NiCo_2O_4$/NF-300.

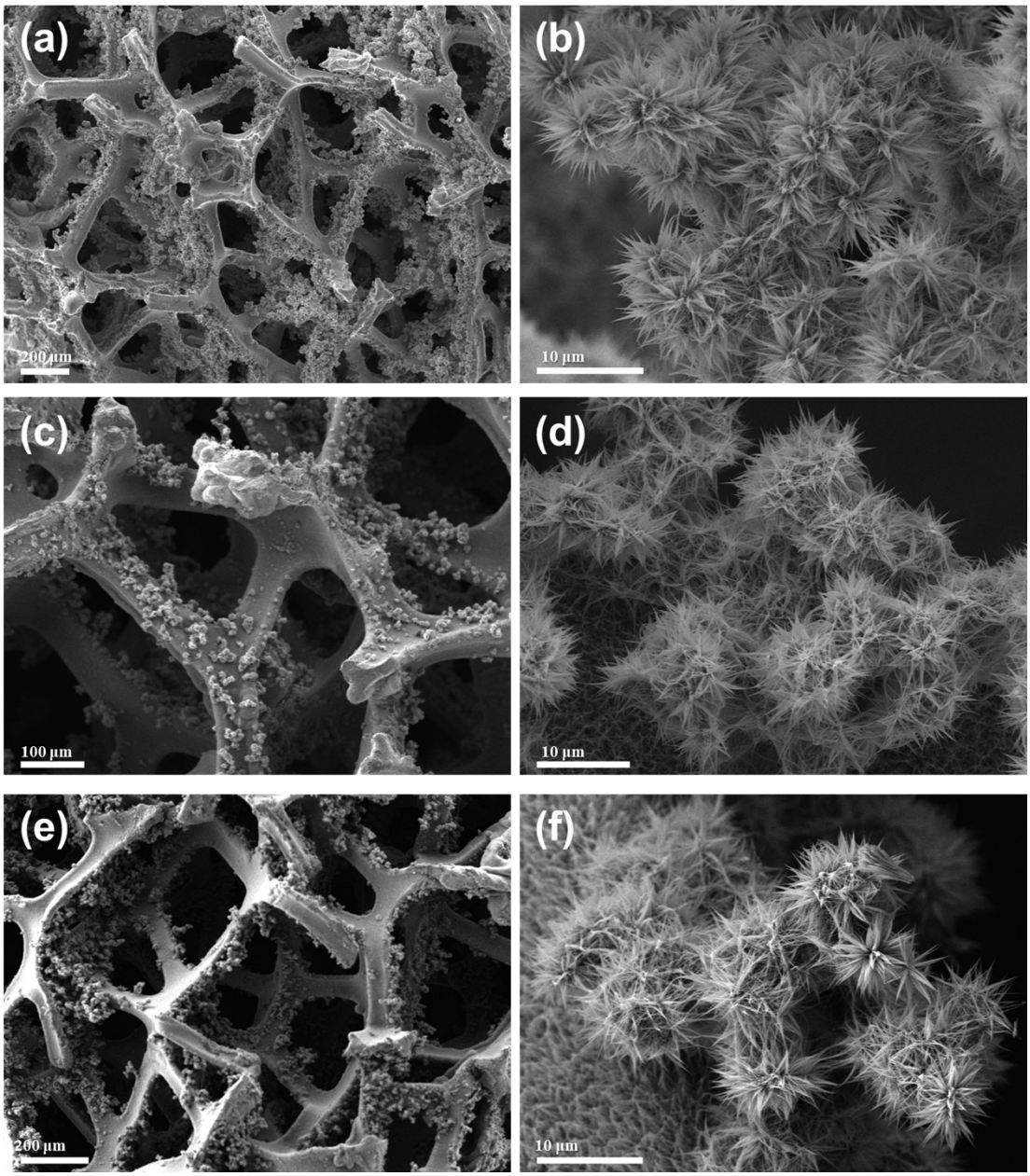

Fig. S8. SEM images of (a, b) $CoNi(OH)_x$/NF, (c, d) NiO/$NiCo_2O_4$/NF-200 and (e, f) NiO/$NiCo_2O_4$/NF-400.

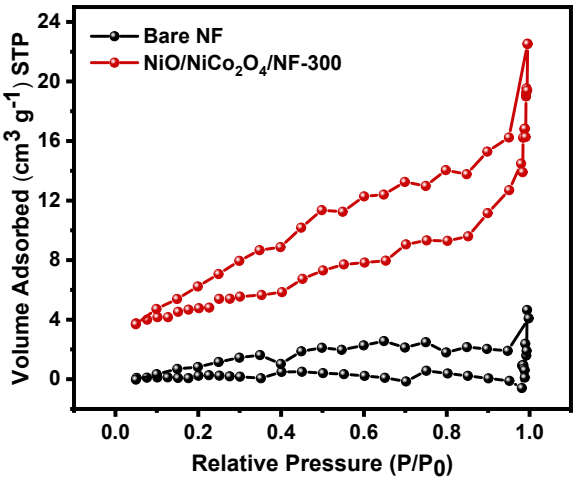

Fig. S9. N_2 adsorption-desorption isotherms of $NiO/NiCo_2O_4$/NF-300 and bare NF.

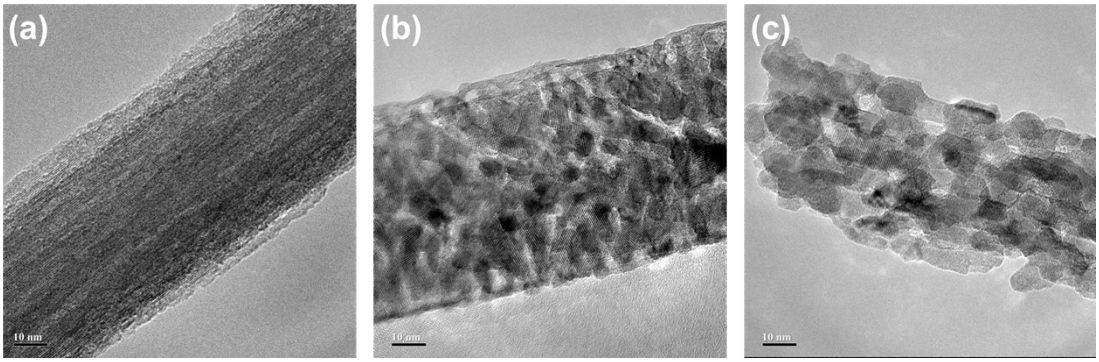

Fig. S10. TEM images of (a) NiO/$NiCo_2O_4$/NF-200, (b) NiO/$NiCo_2O_4$/NF-300 and (c) NiO/$NiCo_2O_4$/NF-400.

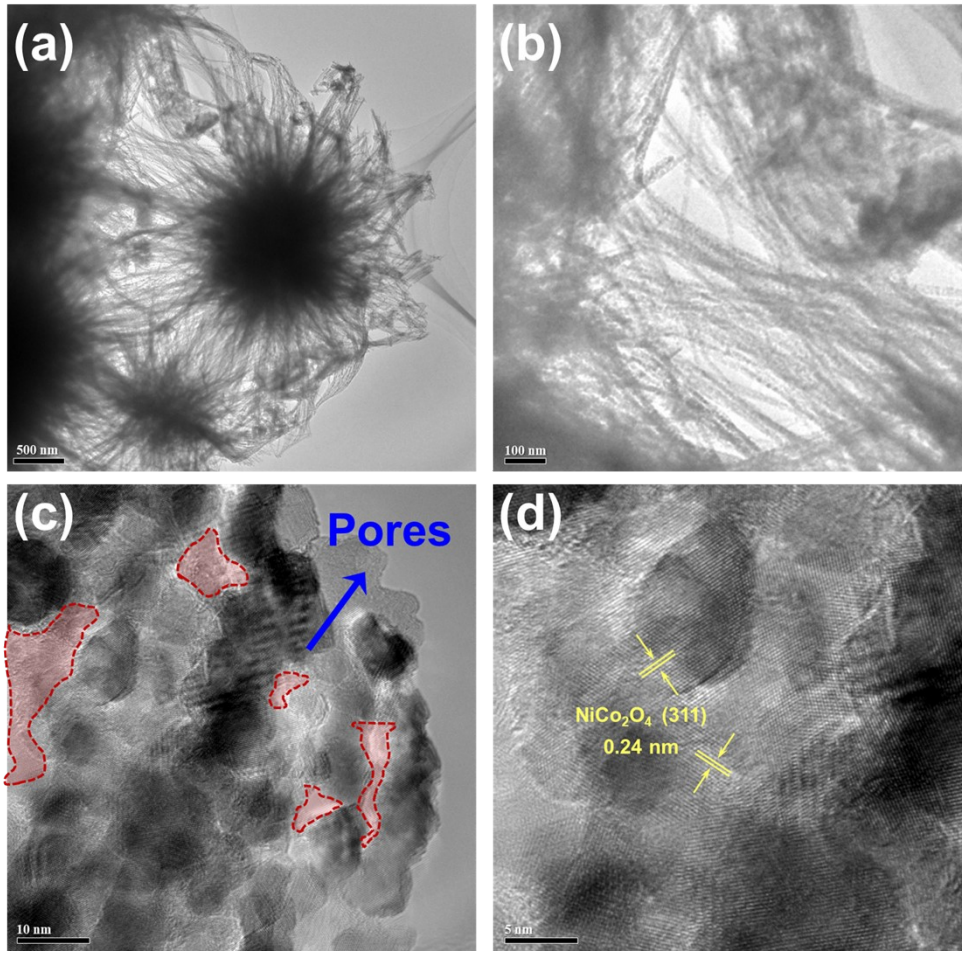

Fig. S11. TEM images of $NiCo_2O_4$.

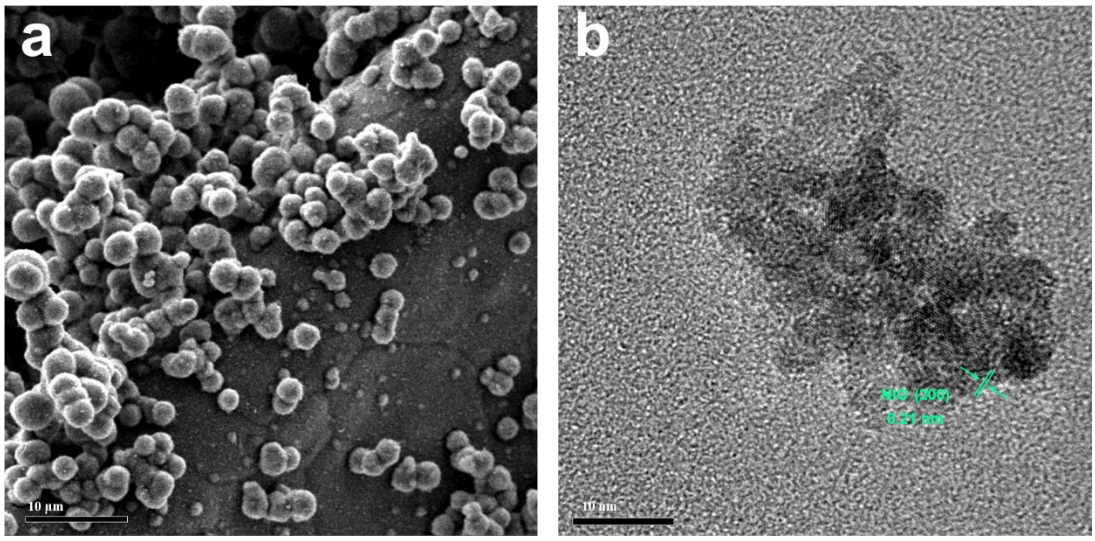

Fig. S12. (a) SEM image and (b) TEM image of NiO/NF.

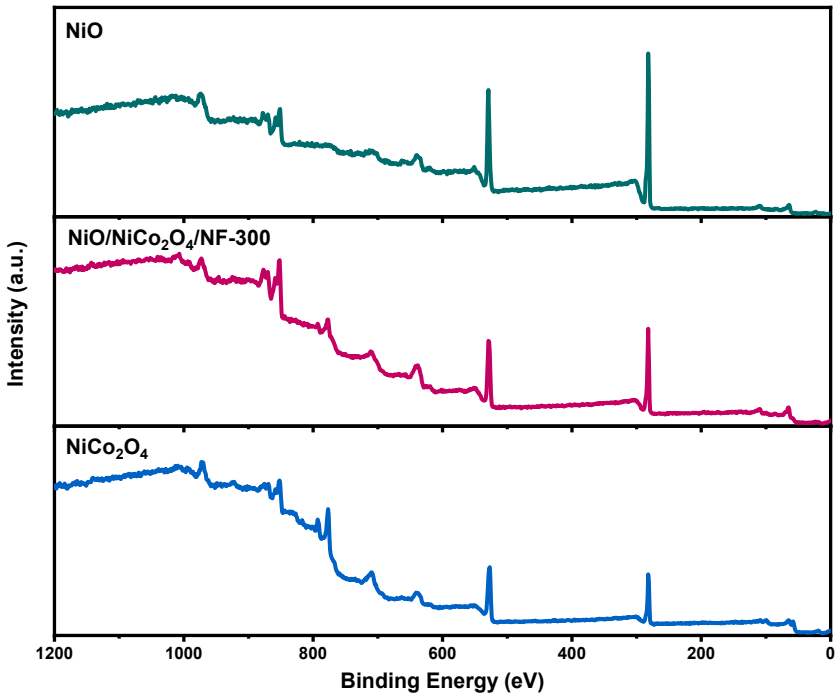

Fig. S13. XPS spectra of $NiCo_2O_4$, $NiO/NiCo_2O_4$/NF-300 and NiO.

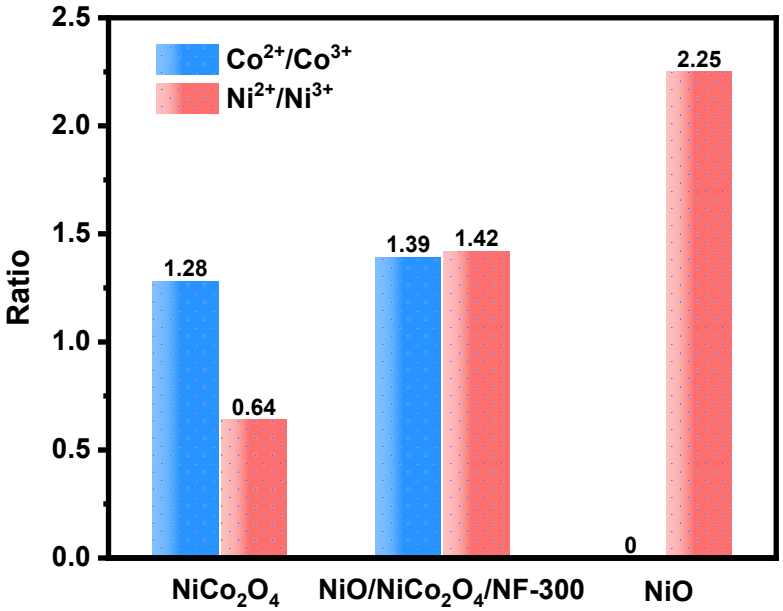

Fig. S14. The Co^{2+}/Co^{3+} and Ni^{2+}/Ni^{3+} ratios obtained from XPS of the corresponding samples.

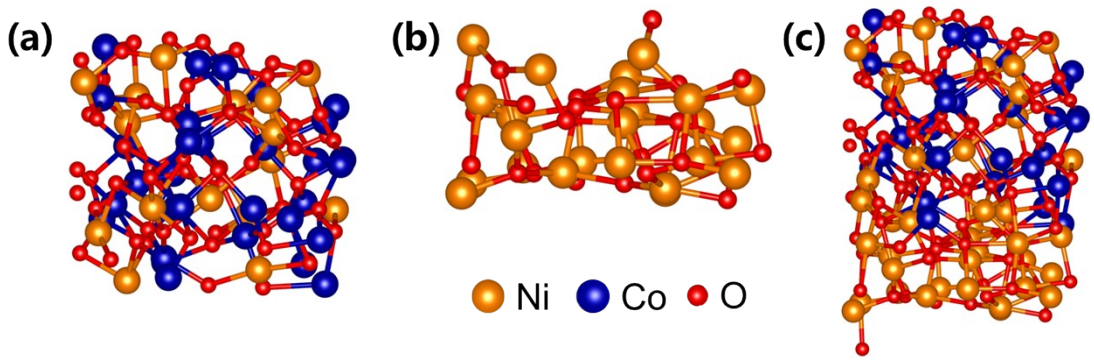

Fig. S15. The theoretical models of the optimized configurations of (a) $NiCo_2O_4$, (b) NiO and (c) $NiO/NiCo_2O_4$ heterojunction.

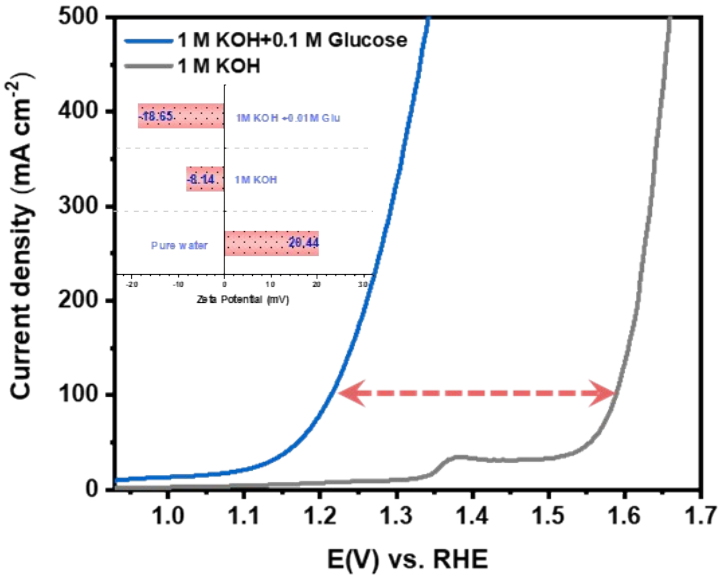

Fig. S16. the corresponding LSV curves of $NiO/NiCo_2O_4$/NF-300 with and without 0.1 M glucose in 1.0 M KOH (inset shows the corresponding zeta potential in different environments).

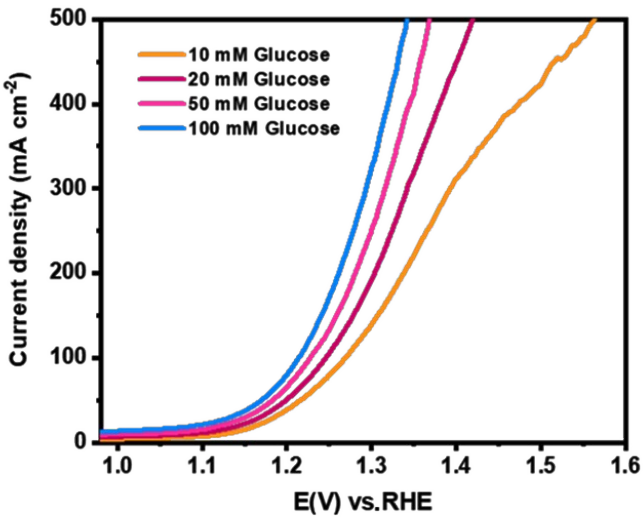

Fig. S17. LSV curves of $NiO/NiCo_2O_4$/NF-300 at different glucose concentrations.

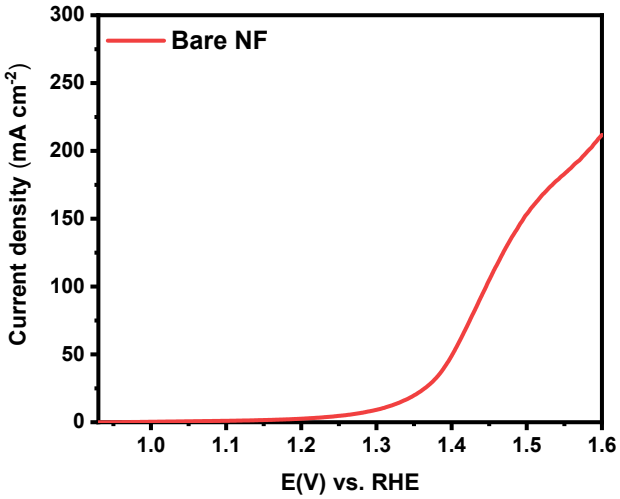

Fig. S18. LSV curves of bare NF with 0.1 M glucose in 1.0 M KOH.

Table S1. Comparison of our catalyst with the reported catalysts for electrochemical saccharides oxidation

Electrocatalyst	Electrolyte	Potential (V *vs*. RHE)	j (mA cm^{-2})	Ref.
$NiFeO_x$-NF	1 M KOH + 50 mM glucose	1.30	61.5	[1]
$Fe_{0.1}$-$CoSe_2$/CC	1 M KOH + 500 mM glucose	1.35	100	[2]
Fe_2P/SSM	1 M KOH + 500 mM glucose	1.33	100	[3]
Ru@Ni-B/NF	1 M KOH + 100 mM glucose	1.24	10	[4]
Co_9S_8/Ni_3S_2	1 M KOH + 50 mM xylose	1.27	100	[5]
NiCoP	1 M KOH + 100 mM xylose	1.29	100	[6]
Ni-MoS_2 NPs	1 M KOH + 300 mM glucose	1.46	10	[7]
NiVP/Pi-VC	1 M KOH + 100 mM glucose	1.3	10	[8]
CNT@Co/CoP	1 M KOH + 500 mM glucose	1.42	10	[9]
Co@NPC	1 M KOH + 100 mM glucose	1.46	10	[10]
$CoWO_4$	1 M KOH + 100 mM glucose	1.44	10	[11]
$NiO/NiCo_2O_4$/NF-300	**1 M KOH + 100 mM glucose**	**0.93** **1.21** **1.34**	**10** **100** **500**	**This work**

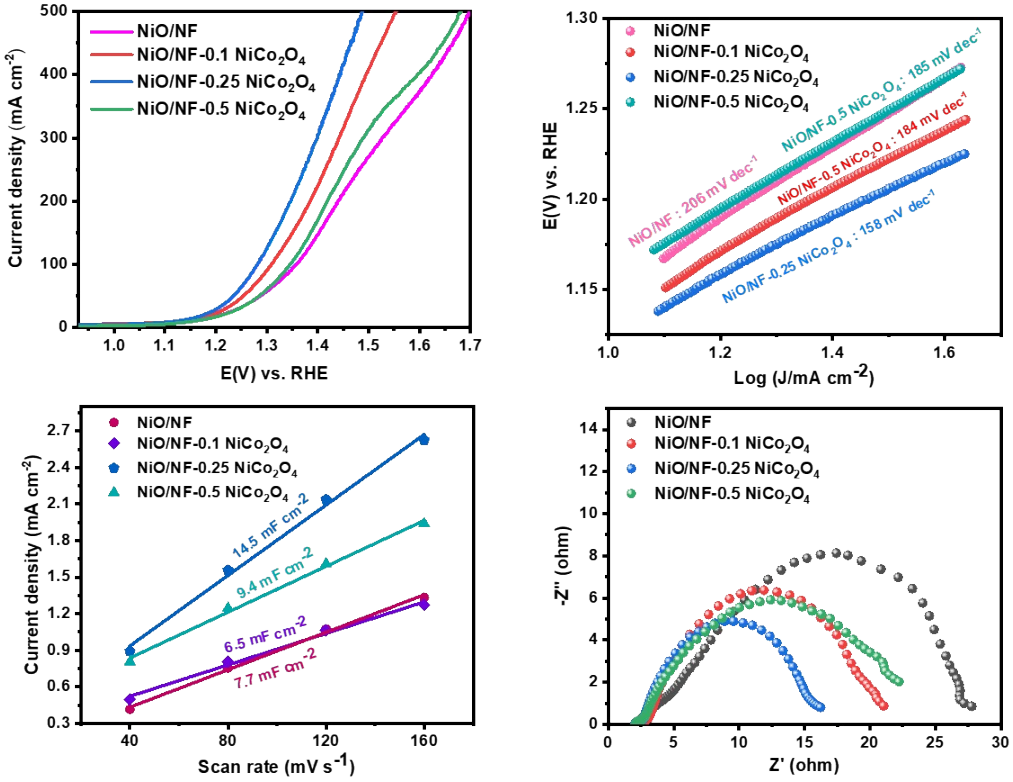

Fig. S19. (a) GOR LSV curves. (b) Tafel plots derived from the LSV curves in (a). (c) Electrochemical double-layer capacitances. (d) Nyquist plots of NiO/NF with different $NiCo_2O_4$ loadings.

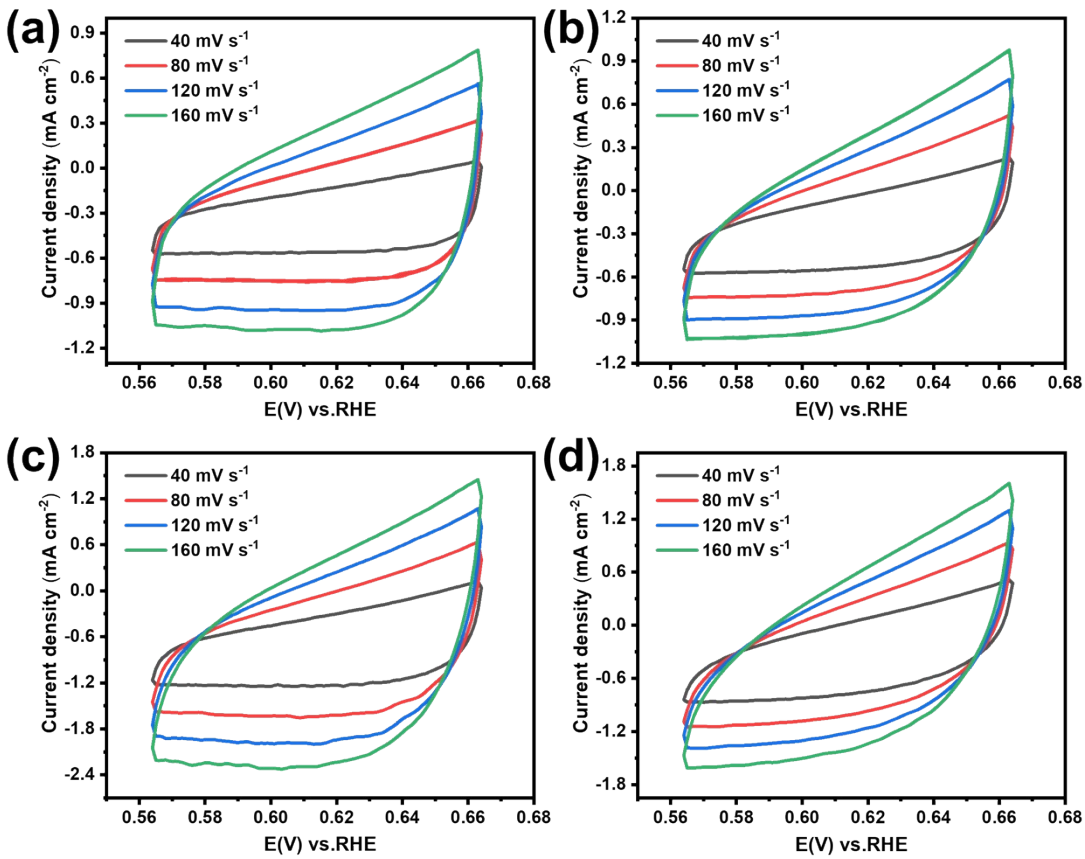

Fig. S20. CV curves of (a) NiO/NF, (b) NiO/NF-0.1 $NiCo_2O_4$ and (c) NiO/NF-0.25 $NiCo_2O_4$ (d) NiO/NF-0.5 $NiCo_2O_4$ at different scan rates.

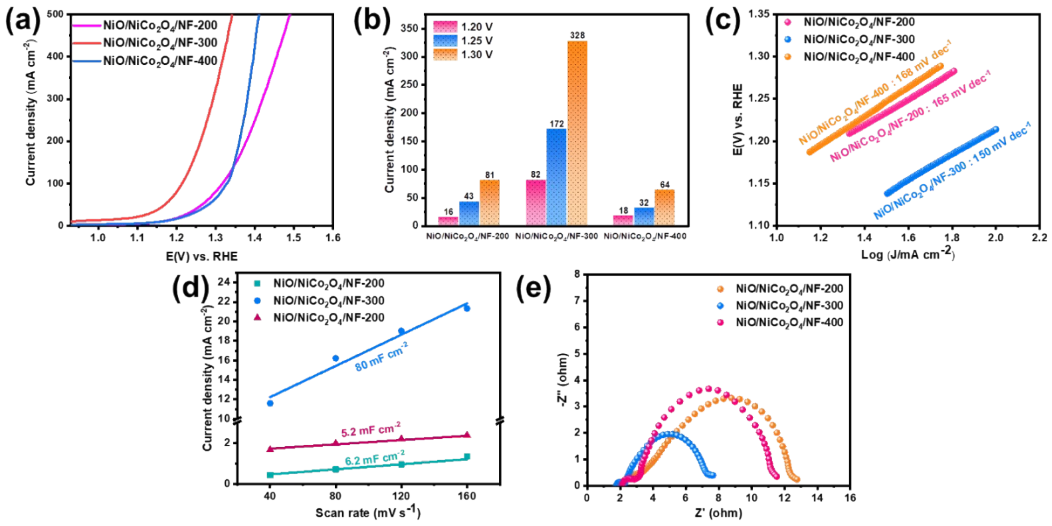

Fig. S21. (a) LSV curves. (b) Corresponding current densities at different potentials. (c) Tafel plots derived from the LSV curves in (a). (d) Electrochemical double-layer capacitances. (e) Nyquist plots of samples obtained at different calcination temperatures.

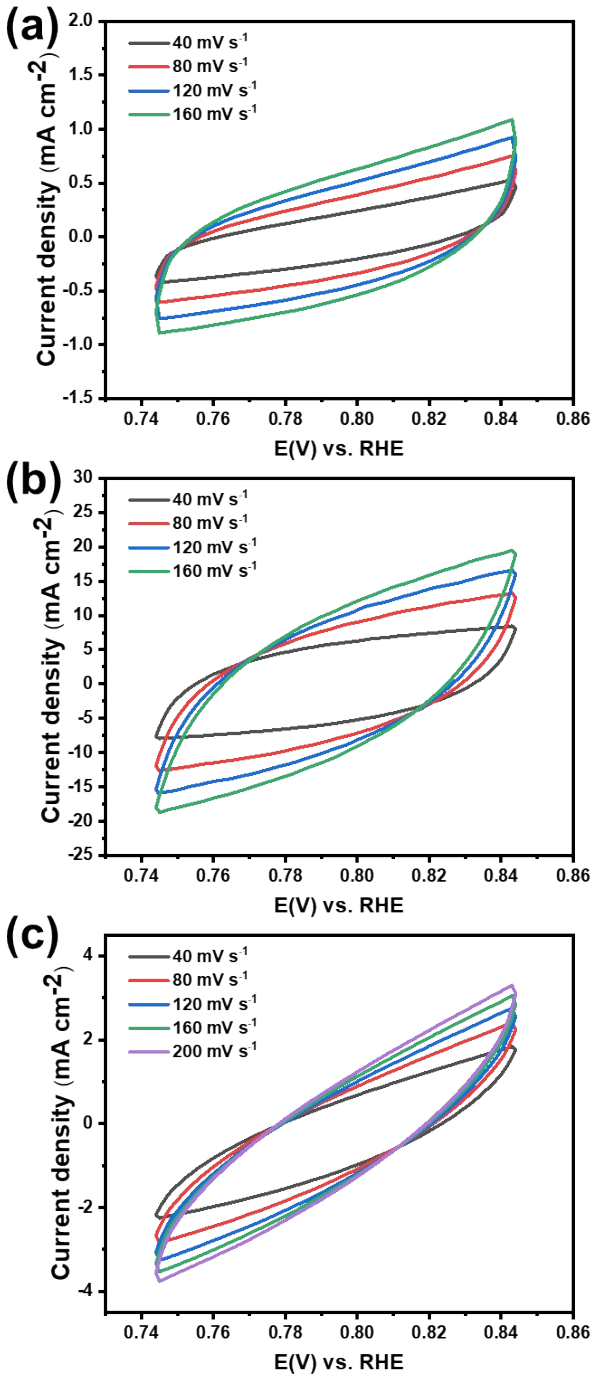

Fig. S22. CV curves of (a) NiO/$NiCo_2O_4$/NF-200, (b) NiO/$NiCo_2O_4$/NF-300 and (c) NiO/$NiCo_2O_4$/NF-400 at different scan rates.

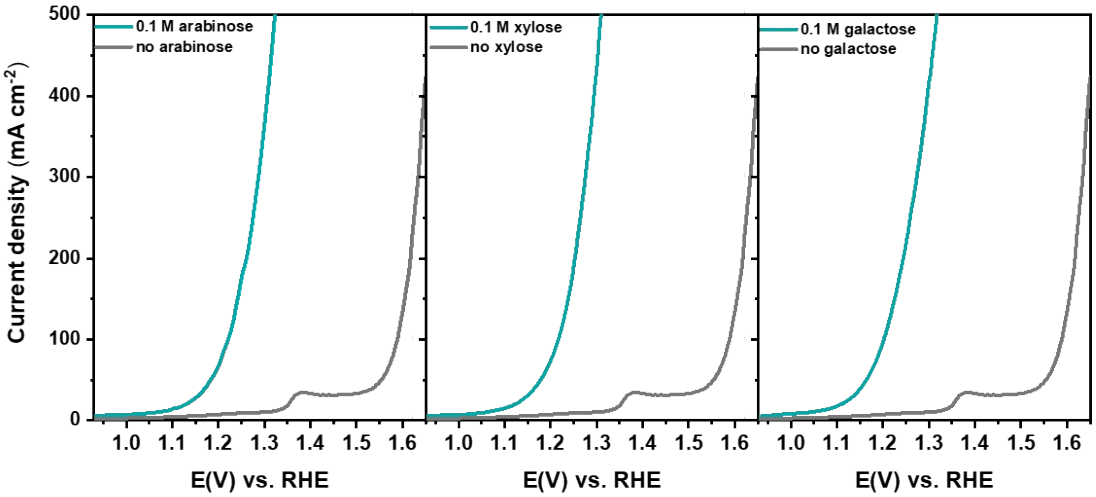

Fig. S23. The corresponding LSV curves of $NiO/NiCo_2O_4$/NF-300 with and without 0.1 M monosaccharide (galactose, xylose, arabinose) in 1.0 M KOH.

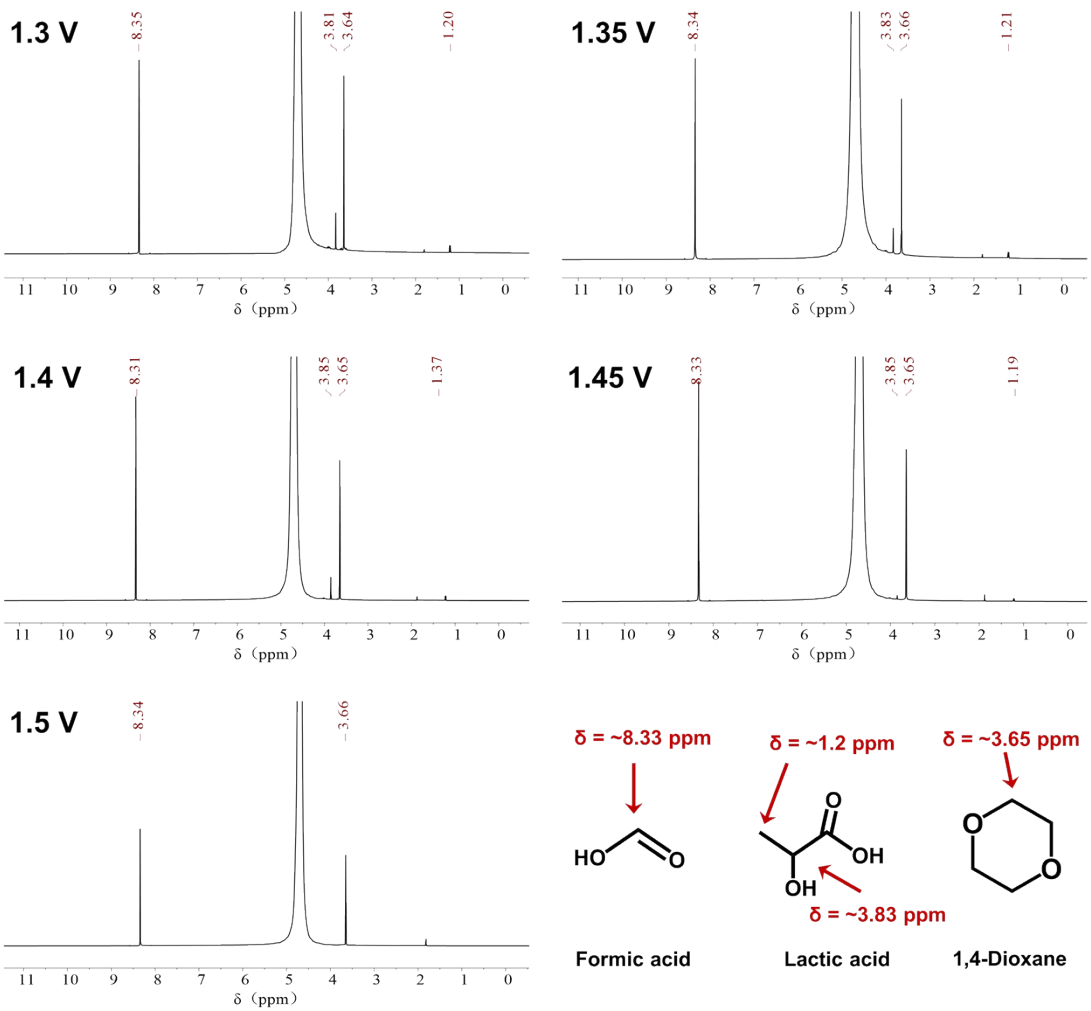

Fig. S24. ^{1}H qNMR spectra of oxidized products in the electrolyte after 12 h electrolysis of glucose at 1.3 V, 1.35 V, 1.4 V, 1.45 V and 1.5 V.

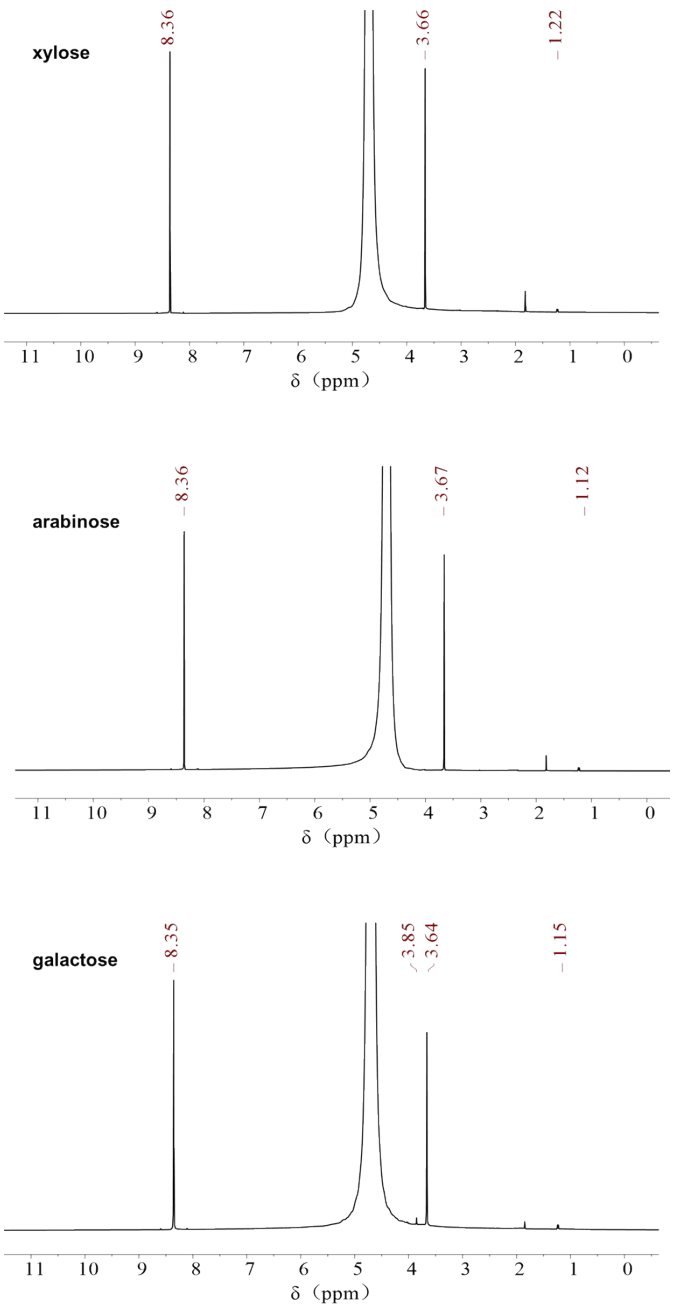

Fig. S25. ^{1}H qNMR spectra of oxidized products of xylose, galactose and arabinose in the electrolyte after electrolysis at 1.35 V for 12 h.

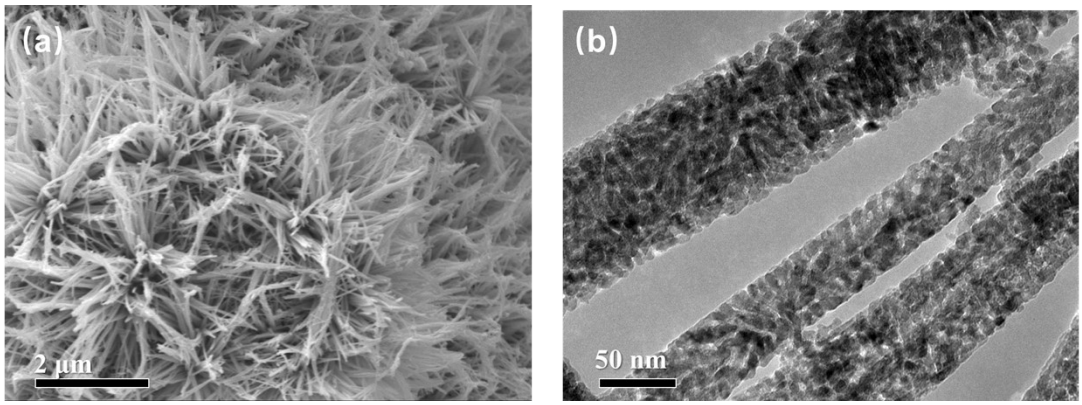

Fig. S26. (a) SEM and (b) TEM image of post-NiO/$NiCo_2O_4$/NF-300.

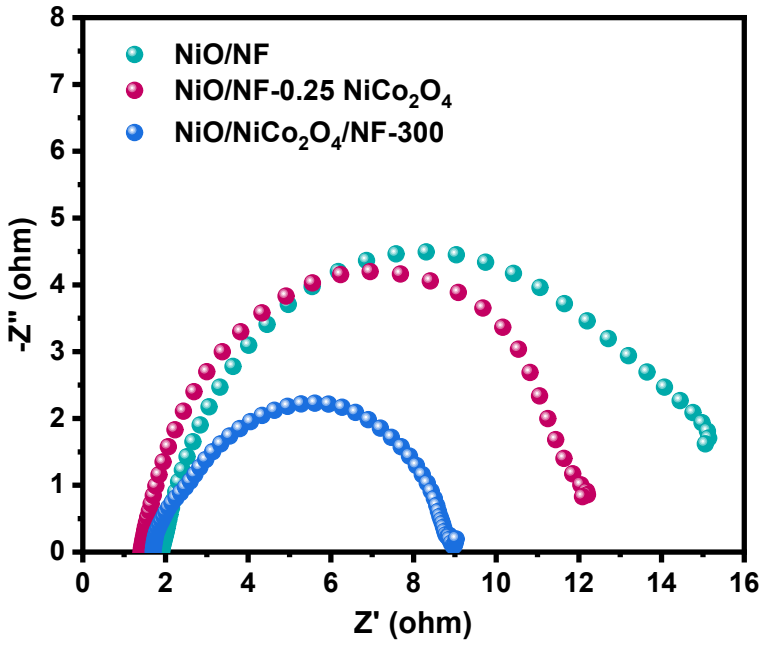

Fig. S27. Nyquist plots of NiO/NF, NiO/NF-0.25 $NiCo_2O_4$ and NiO/$NiCo_2O_4$/NF-300.

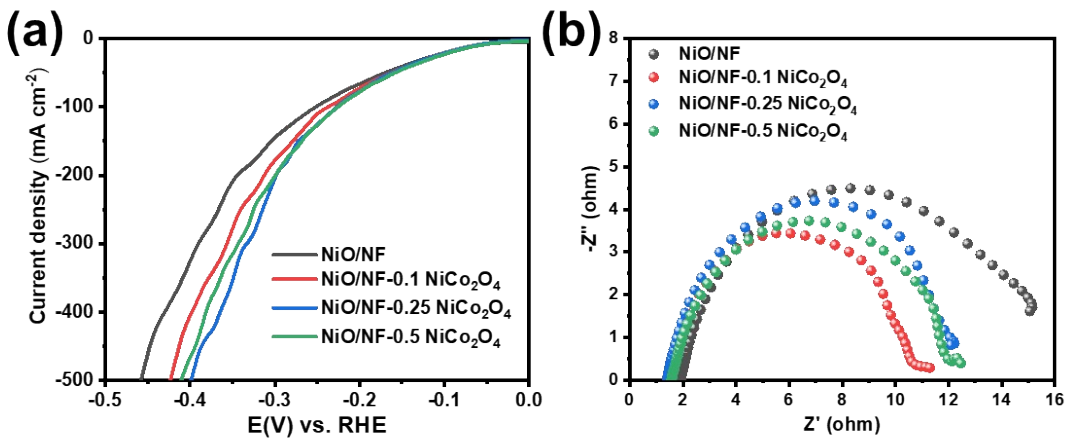

Fig. S28. (a) LSV curves. (b) Nyquist plots of samples with different $NiCo_2O_4$ loadings.

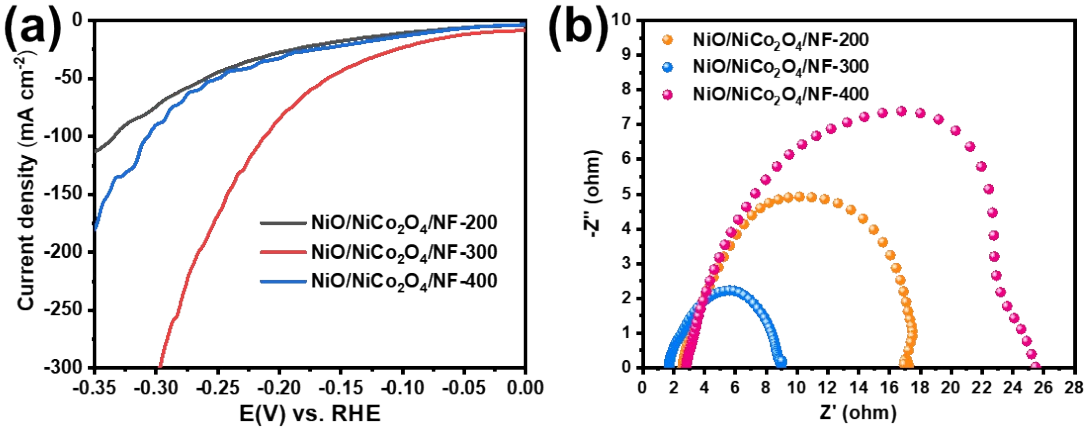

Fig. S29. (a) LSV curves. (b) Nyquist plots of samples obtained at different calcination temperatures.

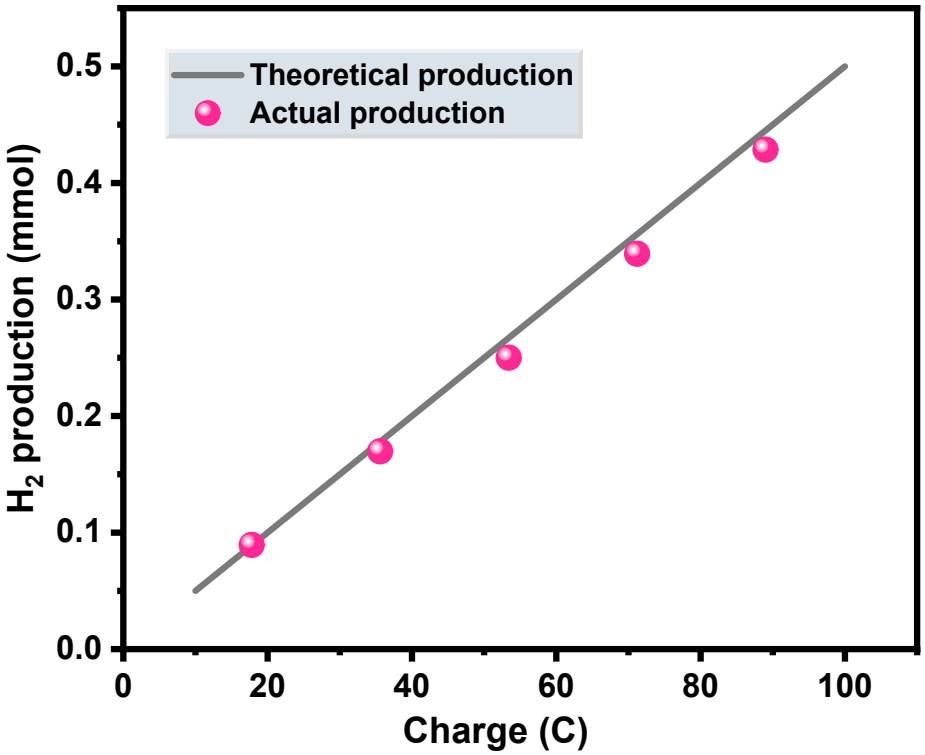

Fig. S30. Actual H_2 production compared with theoretically calculated H_2 production.

References

1. W. J. Liu, Z. Xu, D. Zhao, X. Q. Pan, H. C. Li, X. Hu, Z. Y. Fan, W. K. Wang, G. H. Zhao, S. Jin, G. W. Huber and H. Q. Yu, *Nat. Commun.*, 2020, **11**, 265.
2. D. Zheng, J. Li, S. Ci, P. Cai, Y. Ding, M. Zhang and Z. Wen, *Appl. Catal. B: Environ.*, 2020, **277**, 119178.
3. P. Du, J. Zhang, Y. Liu and M. Huang, *Electrochem. commun.*, 2017, **83**, 11-15.
4. H. Liu, R. Zhang, L. Chen, L. Wang, Y. Guo and Y. Yang, *Adv. Sustain. Syst.*, 2021, **5**, 2000184.
5. Y. Liu, R. Zou, B. Qin, J. Gan and X. Peng, *Chem. Eng. J.*, 2022, **446**, 136950.
6. Y. Yang, R. Zou, J. Gan, Y. Wei, Z. Chen, X. Li, S. Admassie, Y. Liu and X. Peng, *Green Chem.*, 2023, **25**, 4104.
7. X. Liu, P. Cai, G. Wang and Z. Wen, *Int. J. Hydrog. Energy*, 2020, **45**, 32940-32948.
8. N. Thakur, D. Mehta, A. Chaturvedi, D. Mandal and T. C. Nagaiah, *J. Mater. Chem. A*, 2023, **11**, 15868.
9. Y. Zhang, Y. Qiu, Z. Ma, Y. Wang, Y. Zhang, Y. Ying, Y. Jiang, Y. Zhu and S. Liu, *J. Mater. Chem. A*, 2021, **9**, 10893.
10. D. Li, Y. Huang, Z. Li, L. Zhong, C. Liu and X. Peng, *Chem. Eng. J.*, 2022, **430**, 132783.
11. A. Chaturvedi, D. Gupta, S. Kaur, K. Garg and T. C. Nagaiah, *J. Mater. Chem. A*, 2023, **11**, 18280-18290.